

Enhancing inflationary model predictions via refined slow-roll dynamics

Debottam Nandi, Simran Yadav, and Manjeet Kaur

Department of Physics and Astrophysics, University of Delhi, Delhi 110007, India

E-mail: dnandi@physics.du.ac.in, simranyadavkhola@gmail.com,
mkaur1@physics.du.ac.in

Abstract. The inflationary paradigm not only addresses early Universe puzzles but also aligns well with the observational constraints, with slow-roll inflationary models fitting best. Evaluating these model predictions requires considering both slow-roll inflationary dynamics and the subsequent reheating epoch. This involves the quantitative analysis that takes into account the effective equation of state (EoS) and duration of reheating, connecting these with the perturbations generated deep during the inflationary era. Given the complexities involved, many approximations are often used for simplification. However, as future observations are expected to improve the accuracy of these observables significantly, this work takes a different approach. Instead of relying on approximations, we consider the near-accurate solutions of inflationary models and compare our results with the pre-existing ones. It mainly incorporates two improvements: the first is the accurate dynamics of the slow-roll evolution, and, thus, the end of inflation; and the second is the higher-order slow-roll corrections to the perturbed observables. Our findings indicate that, by implementing these corrections, the theoretical predictions improve significantly. It also indicates that seemingly minor corrections can have significant effects on the perturbed observables and these refined predictions can be compared with future observations to potentially rule out models and help resolve the degeneracy problem of the inflationary paradigm.

Keywords: The Early Universe, Inflationary Paradigm, Reheating, CMBR, Perturbations.

Contents

1	Introduction	1
2	General equations and slow-roll conditions	3
3	Quantitative analysis of reheating	5
3.1	Starobinsky inflation	6
4	Numerical improvements	10
4.1	Implementation of accurate inflationary dynamics through numerical methods	11
4.2	Implementation of higher-order slow-roll approximations	14
4.3	Implementation of the onset of reheating as the bottom of the potential	17
5	Summary and conclusions	18

1 Introduction

The inflationary paradigm [1–31], which describes a brief period of accelerated expansion, is the most successful framework for explaining the dynamics of the early Universe. Within this paradigm, slow-roll inflation involves field(s) slowly rolling down the potential, resulting in near-exponential expansion and providing an explanation for the observational constraints [32–35]. As the field(s) approaches the bottom of the potential, inflation ends, and shortly afterward, the field(s) begins to oscillate around this minimum. This phase, known as the reheating epoch, involves the inflaton field(s) coupling with and decaying into other standard particles, leading to the onset of the radiation-dominated era [36–58].

Theoretical constraints derived from an inflationary model, however, not only depend on the dynamics of inflation itself but also depend on the reheating era, and therefore, studying reheating dynamics is crucial for accurately predicting the early Universe behavior. There are two main approaches to this: the first is the qualitative analysis [36–43, 46] which examines the exact decay process of the inflaton field through the parametric resonance, leading to the understanding of the microphysics involved during the reheating epoch. The second approach, which is the main focus of this manuscript, is the quantitative analysis [44, 45, 47, 49, 52, 54, 59–63]. This approach looks at the macrophysics of the reheating epoch by constraining the duration (N_{re}) and the equation of state (EoS) parameter (w_{re}) during the reheating era using perturbations generated deep in the early (inflation) Universe.

In this analysis, the Hubble horizon and the associated length scales are used to constrain the duration when the pivot scale exits the Hubble horizon from the end of inflation, i.e., N_k , and the reheating parameters (N_{re} , w_{re}). Given any model, using N_k , one can determine both the scalar and tensor perturbations associated with the pivot scale and compare this with the observations. Thus, the theoretically obtained perturbed observables, namely the scalar-spectral index n_s and the tensor-to-scalar ratio r are heavily dependent on the reheating parameters N_{re} and w_{re} . Since the perturbations (n_s and r) are highly sensitive to N_k , and consequently, to (N_{re} , w_{re}), even small corrections or deviations in N_k or reheating parameters can significantly improve n_s . Ongoing experiments [32–35] already measure n_s with an accuracy of $\Delta n_s \sim 10^{-2}$ and upcoming experiments like PRISM [64], EUCLID [65],

cosmic 21-cm surveys [66], and CORE experiments [67] are projected to improve this accuracy to $\Delta n_s \sim 10^{-3}$. Therefore, taking advantage of this, in this work, we focus on refining the analysis itself to obtain tighter constraints on the inflationary paradigm, as the analysis relies on numerous approximations. This refined approach, in turn, can help resolve the degeneracy problem of the inflationary paradigm [25, 68–70] by eliminating more inflation models.

Improving the analysis can again be performed in two main ways. The first one involves a detailed and careful consideration of the reheating analysis that can accurately depict the reheating parameters $(N_{\text{re}}, w_{\text{re}})$. However, since it entails dealing with various distinct micro-physical processes, i.e., the qualitative analysis, we have opted not to pursue this approach as it is beyond the scope of this work. Instead, we focus on the second, more straightforward improvement: the slow-roll methodology and approximations. Recent findings in Refs. [71, 72] indicate that a near-accurate analytical solution can significantly enhance background predictions near the end of inflation, thereby improving N_k [71]. For example, in the case of Starobinsky inflation, the improvement $\Delta N_k \sim 1.5$ suggests that

$$n_s \sim 1 - \frac{2}{N_k}, \quad \Delta n_s \sim \frac{\Delta N_k}{N_k^2} \sim 10^{-3}.$$

In addition to leading-order slow-roll approximations, higher-order slow-roll corrections [73–87] can be considered to further improve the evaluation of perturbed observables such as n_s and r . Therefore, the objective of this work is to enhance the model predictions by implementing both the improved near-accurate dynamics and higher-order slow-roll corrections and comparing our results with the existing literature. As an example, we consider the most popular inflationary model: the Starobinsky model of inflation [1, 2, 8, 88, 89]. Using the conventional leading order analytical approximation, the constraint on n_s is: $0.9613 \leq n_s \leq 0.9641$, which leads to further constrain $N_{\text{re}} \leq 16$ (equivalently, the energy at the end of reheating, i.e., $T_{\text{re}} \geq 10^{10}$ GeV, assuming $w_{\text{re}} = 0$). However, after implementing the accurate dynamics as well as the higher-order slow-roll corrections, the bounds on these parameters change significantly, and the new constraint on n_s for numerical solution becomes: $0.9613 \leq n_s \leq 0.9649$, which leads to further constrain $N_{\text{re}} \leq 21$ (and subsequently, $T_{\text{re}} \geq 10^8$ GeV), while for higher-order corrections these become: $0.9613 \leq n_s \leq 0.9653$, constraints on reheating parameters are, $N_{\text{re}} \leq 24$ and $T_{\text{re}} \geq 10^7$, which has the potential to rule out the model from future observations. The result is unexpected, as one might anticipate the corrections to be negligible. Thus, instead of relying on the conventional approximation method, our results demonstrate the critical need for corrections due to the accurate dynamics in each model of inflation, which may lead to a significant change in theoretical predictions and potentially rule out models from observations. This implies that even seemingly minor improvements to the background dynamics can have a substantial impact on the theoretically obtained perturbed observables, which must not be ruled out without verification.

The article is structured as follows: the following section 2 presents the model and the subsequent dynamics for the early Universe dynamics. In this section, we also demonstrate the slow-roll conditions as well as the slow-roll approximations. In the subsequent section 3, we study the quantitative analysis of reheating linking the inflationary perturbed variables to the observable constraints. This section, as an example, also examines the popular Starobinsky model of inflation, and with the help of the reheating analysis along with leading-order slow-roll approximations, we carefully obtain the observational consequences of the model. In Sec. 4, we highlight the dire need for the corrections to the dynamics, subsequently im-

plement these changes, and obtain the improved constraint of the model, which turns out to be significant. Finally, we conclude our work in Sec. 5.

A brief explanation about some terms and symbols we'll be using. In our work, we use natural units where $\hbar = c = k_B = 1$. We also define the reduced Planck mass as $M_{\text{pl}} \equiv (8\pi G)^{-1/2} = 1$. The metric signature we use is $(-, +, +, +)$. Greek indices are contracted with the metric tensor $g_{\mu\nu}$, while Latin indices will be contracted with the Kronecker delta δ_{ij} . We use symbols ∂ and ∇ for partial and covariant derivatives, respectively. Additionally, the dots and primes above symbols represent derivatives for cosmic and conformal time, respectively, related to the Friedmann-Lemaître-Robertson-Walker (FLRW) line-element.

2 General equations and slow-roll conditions

In this section, we discuss the general equations and solutions for a slow-roll inflationary Universe. For that, let us consider the simplest action with a single canonical scalar field ϕ minimally coupled to gravity with a potential $V(\phi)$, which can be written as

$$S = \frac{1}{2} \int d^4x \sqrt{-g} (R - g^{\mu\nu} \partial_\mu \phi \partial_\nu \phi - 2V(\phi)). \quad (2.1)$$

Here, R is the Ricci scalar. The corresponding equations of motion, i.e., Einstein's equations and the equation of the scalar field, can be written as

$$R_{\mu\nu} - \frac{1}{2} g_{\mu\nu} R = T_{\mu\nu(\phi)}, \quad (2.2)$$

$$\nabla_\mu T^{\mu\nu}_{(\phi)} = 0, \quad (2.3)$$

where $T^{\mu}_{\nu(\phi)}$ is the stress-energy tensor corresponding to the ϕ field and can be written as

$$T_{\mu\nu(\phi)} = \partial_\mu \phi \partial_\nu \phi - g_{\mu\nu} \left(\frac{1}{2} \partial_\lambda \phi \partial^\lambda \phi + V(\phi) \right). \quad (2.4)$$

Using the flat FLRW line element describing the homogeneous and isotropic Universe at large scales, i.e.,

$$ds^2 = -dt^2 + a^2(t) d\mathbf{x}^2, \quad (2.5)$$

where, $a(t)$ is the scalar factor, Eqs. (2.2) and (2.3) can be reduced to

$$3H^2 = \frac{1}{2} \dot{\phi}^2 + V(\phi), \quad (2.6)$$

$$\dot{H} = -\frac{1}{2} \dot{\phi}^2, \quad (2.7)$$

$$\ddot{\phi} + 3H\dot{\phi} + V_{,\phi} = 0. \quad (2.8)$$

where, $H \equiv \dot{a}/a$ is the Hubble parameter, and $A_x \equiv \partial A / \partial x$. These equations can be re-defined in terms of the e-fold variable $N \equiv \int H dt = \ln(a/a_0)$ as

$$H = \sqrt{\frac{V}{3 - \frac{1}{2} \phi_N^2}}, \quad \frac{H_N}{H} = -\frac{1}{2} \phi_N^2, \quad (2.9)$$

$$\phi_{NN} + \left(3 - \frac{1}{2} \phi_N^2 \right) \left(\phi_N + \frac{V_{,\phi}}{V} \right) = 0, \quad (2.10)$$

where, $A_{xx} = \partial^2 A / \partial x^2$. Given a potential $V(\phi)$, one can solve the above equations to correctly obtain the dynamics of the early Universe. Once the background equations are solved, one can in principle, solve the scalar (\mathcal{R}_k) and tensor (h_k) perturbations and evaluate the power spectra:

$$\mathcal{P}_{\mathcal{R}} = \frac{k^3}{2\pi^2} |\mathcal{R}_k|^2 \equiv A_{\mathcal{R}} \left(\frac{k}{k_*} \right)^{n_s-1}, \quad \mathcal{P}_T = 2 \frac{k^3}{2\pi^2} |h_k|^2 \equiv A_T \left(\frac{k}{k_*} \right)^{n_T} \quad (2.11)$$

where, k_* is the pivot scale, $A_{\mathcal{R}}$, A_T are the scalar and tensor spectral amplitude,

$$n_s \equiv \left. \frac{d \ln \mathcal{P}_{\mathcal{R}}}{d \ln k} \right|_{k=k_*}, \quad n_T \equiv \left. \frac{d \ln \mathcal{P}_T}{d \ln k} \right|_{k=k_*}$$

are the scalar and tensor spectral index and and

$$r \equiv \frac{A_T}{A_{\mathcal{R}}}$$

is defined as the tensor-to-scalar ratio, which we compare with the observations. The current observations (PLANCK [32, 33, 35], BICEP/Keck [34]) suggest that, at the pivot scale ($k_* = 0.05 \text{ Mpc}^{-1}$), the amplitude of the scalar power spectrum is $A_{\mathcal{R}} \simeq 2.101_{-0.034}^{+0.031} \times 10^{-9}$ (68% CL) with the scalar spectral index being $n_s = 0.9672 \pm 0.0059$ (68% CL), while the ratio (r) of the tensor-to-scalar perturbation amplitudes is bounded by $r < 0.028$ (95% CL). These observations agree remarkably well with the predictions of a near-scale-invariant spectrum of density perturbations in the inflationary paradigm. In the next section, we will discuss in detail, how, without explicitly evaluating the perturbations, one can obtain these observables using the background solutions in the case of slow-roll inflation.

Slow-roll inflation

Let us first define the two slow-roll parameters ϵ_1 and ϵ_2 as

$$\epsilon_1 \equiv -\frac{\dot{H}}{H^2} = \frac{1}{2} \phi_N^2, \quad \epsilon_2 \equiv \frac{\dot{\epsilon}_1}{H \epsilon_1} = 2 \frac{\phi_{NN}}{\phi_N}. \quad (2.12)$$

The first variable $\epsilon_1 < 1$ ensures that the Universe is accelerating. On the other hand, the second variable $\epsilon_2 \ll 1$ ensures the sufficient duration of the inflationary phase. In the case of slow-roll, both these parameters are extremely small, i.e.,

$$\epsilon_1 \ll 1, \quad \epsilon_2 \ll 1. \quad (2.13)$$

These two conditions are also referred to as slow-roll conditions. Under these conditions, Eqs. (2.9) and (2.10) become

$$H^2 \simeq \frac{1}{3} V, \quad \phi_N \simeq -\frac{V_\phi}{V}, \quad (2.14)$$

and the slow-roll parameters can be re-expressed in terms of the shape of the potential as

$$\epsilon_1 \simeq \frac{1}{2} \left(\frac{V_\phi}{V} \right)^2, \quad \epsilon_2 \simeq 2 \left(\frac{V_\phi^2}{V^2} - \frac{V_{\phi\phi}}{V} \right). \quad (2.15)$$

Eqs. (2.14) are referred to as the slow-roll equations. By solving these simplified equations, one can obtain the approximate analytical solution of the Hubble parameter as well as the slow-roll parameters, and thus the dynamics of the Universe in slow-roll regime.

In order to check for consistency with the observation, one can, in principle, obtain the observables corresponding to the perturbations associated with the pivot scale k in terms of slow-roll parameters as

$$A_{\mathcal{R}} \simeq \frac{H^2}{8\pi^2\epsilon_1}, \quad n_s \simeq 1 - 2\epsilon_1 - \epsilon_2, \quad r \simeq 16\epsilon_1. \quad (2.16)$$

The above expressions are obtained using leading-order slow-roll approximation, assuming the higher-order contributions are heavily suppressed. Please note that these observables depend on the time variable N_k , representing the duration between the end of inflation and the epoch when the pivot scale k leaves the Hubble horizon. Typically, this duration is considered to be $N_k \sim 50 - 60$. However, it is a model-dependent quantity and in order to obtain the exact duration N_k , one must consider the post-inflationary dynamics, i.e., the reheating epoch. In the very next section, we will focus on this, which is also known as the quantitative analysis of reheating.

3 Quantitative analysis of reheating

As mentioned in the previous section, in the slow-roll regime, the slow-roll parameters are very small, i.e., $\epsilon_1, \epsilon_2 \ll 1$. However, as the field rolls down the potential, these slow-roll parameters increase, and the inflation ends as soon as this condition is violated, i.e., $\epsilon_1 = 1$. Briefly, after the end of inflation, the field reaches the bottom and begins to oscillate around it and couples with the other (standard) particles. As a consequence, at this stage, the time average of kinetic energy is the same as the average of the potential energy, and the field decays. This epoch is known as the reheating phase.

To quantify the effect of reheating, let us first simplify it by parametrizing the reheating epoch using an effective EoS parameter w_{re} , such that the energy density during reheating effectively behaves as

$$\rho \propto a^{-3(1+w_{\text{re}})}. \quad (3.1)$$

We also define the duration of reheating N_{re} as

$$N_{\text{re}} \equiv \ln \left(\frac{a_{\text{re}}}{a_{\text{end}}} \right) \quad (3.2)$$

where $a_{\text{end}}, a_{\text{re}}$ are the scale factor solutions at the end of the inflation and reheating epoch, respectively. In order to calculate the duration N_{re} , let us compare the mode of interest with the present scale as

$$\frac{k}{a_0 H_0} = \frac{a_k H_k}{a_0 H_0} = \frac{a_k}{a_{\text{end}}} \frac{a_{\text{end}}}{a_{\text{re}}} \frac{a_{\text{re}}}{a_{\text{eq}}} \frac{a_{\text{eq}}}{a_0} \frac{H_k}{H_{\text{eq}}} \frac{H_{\text{eq}}}{H_0}, \quad (3.3)$$

where k is the comoving scale, and (eq) and (0) denote the quantities at the matter-radiation equality and the present epoch, respectively. Then the above equation leads to:

$$\ln \left(\frac{k}{a_0 H_0} \right) = -N_k - N_{\text{re}} - N_{\text{RD}} + \ln \left(\frac{a_{\text{eq}} H_{\text{eq}}}{a_0 H_0} \right) + \ln \left(\frac{H_k}{H_{\text{eq}}} \right), \quad (3.4)$$

where $N_k \equiv \ln\left(\frac{a_k}{a_{\text{end}}}\right)$, $N_{\text{RD}} \equiv \ln\left(\frac{a_{\text{re}}}{a_{\text{eq}}}\right)$. At the end of reheating, the energy density is

$$\rho_{\text{re}} = \frac{\pi^2}{30} g_{\text{re}} T_{\text{re}}^4 \quad (3.5)$$

where, g_{re} is the effective number of relativistic species upon thermalization. Radiation drives the ensuing expansion, with non-relativistic matter and dark energy making recent additions. Assuming a negligible entropy shift following T_{re} , the current CMB and neutrino background both retain the reheating entropy, which leads to the relation,

$$g_{\text{s, re}} T_{\text{re}}^3 = \left(\frac{a_0}{a_{\text{re}}}\right)^3 \left(2T_0^3 + 6 \times \frac{7}{8} T_{\nu 0}^3\right), \quad (3.6)$$

where the present (CMB) temperature, $T_0 \simeq 2.73$ K, the neutrino temperature, $T_{\nu 0} = (4/11)^{1/3} T_0$, and $g_{\text{s, re}}$ is the effective number of species for entropy at reheating. Therefore, T_{re} can be written as the present temperature T_0 as

$$\frac{T_{\text{re}}}{T_0} = \frac{a_0}{a_{\text{eq}}} \frac{a_{\text{eq}}}{a_{\text{re}}} \left(\frac{43}{11g_{\text{s, re}}}\right)^{1/3}, \quad (3.7)$$

and the Eq. (3.4) can be re-written as

$$N_{\text{re}} = \frac{4}{1 - 3w_{\text{re}}} \left(-N_k - \frac{1}{4} \ln\left(\frac{30}{\pi^2 g_{\text{re}}}\right) - \frac{1}{3} \ln\left(\frac{11g_{\text{s, re}}}{43}\right) - \ln\left(\frac{k}{a_0 T_0}\right) - \frac{1}{4} \ln \rho_{\text{end}} + \ln H_k\right). \quad (3.8)$$

and T_{re} can be reduced to the following form:

$$T_{\text{re}} = \frac{a_0 T_0}{k} \left(\frac{43}{11g_{\text{s, re}}}\right)^{1/3} H_k e^{-N_k - N_{\text{re}}}. \quad (3.9)$$

where H_k can be written as

$$H_k = \frac{\pi \sqrt{r A_{\mathcal{R}}}}{\sqrt{2}}. \quad (3.10)$$

Please note that the Hubble parameter H_k is a function of duration N_k , and therefore, N_{re} is eventually a function of N_k . As spectral index n_s (or any time-dependent parameters like the field ϕ or tensor-to-scalar ratio r) depends on N_k , considering $\{g_{\text{re}}, g_{\text{s, re}}\} \sim 100$, one can plot n_s vs. N_{re} (or T_{re} from the above expression) and obtain strict constraint on N_{re} [25, 47, 53, 55, 59, 90, 91] as n_s is strictly bounded. This is referred to as the quantitative analysis of reheating. In the next section, we will elaborately discuss this analysis by implementing it on the Starobinsky model of inflation.

3.1 Starobinsky inflation

One of the most successful models of slow-roll inflation is the Starobinsky model [1, 2, 8, 88, 89] where the potential in the Einstein frame is given by:

$$V(\phi) = \frac{3}{4} M^2 \left(1 - e^{-\sqrt{2/3}\phi}\right)^2, \quad (3.11)$$

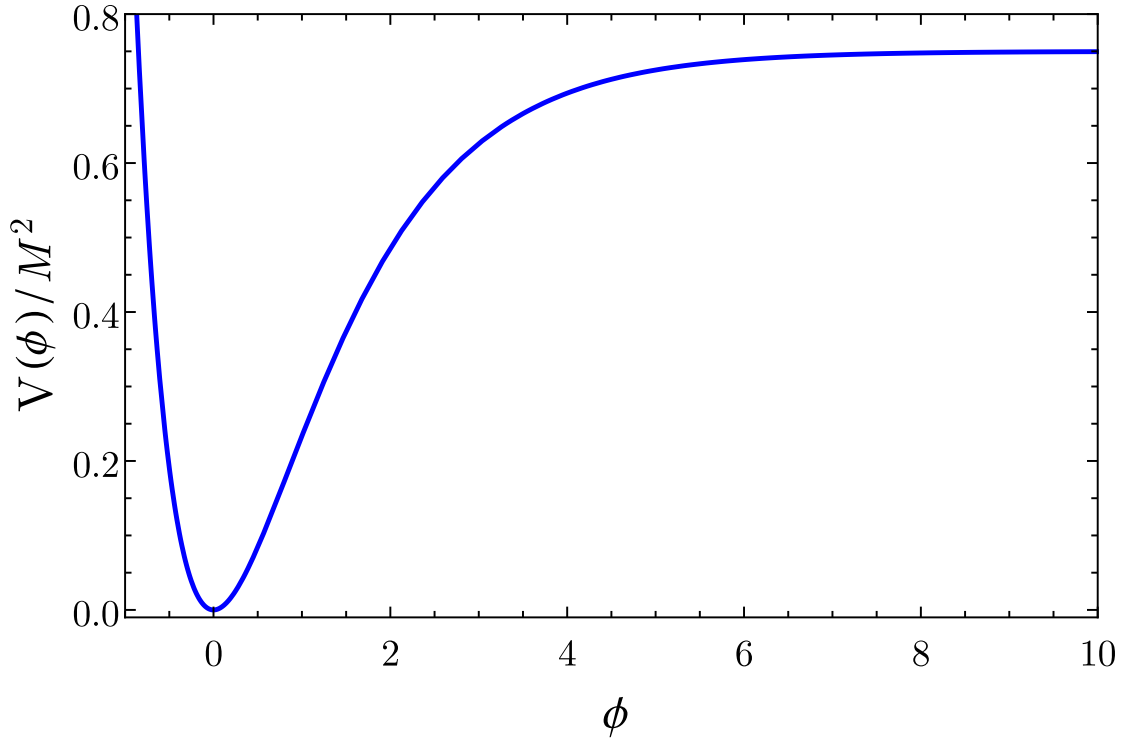


Figure 1: The Starobinsky potential given in Eq. (3.11).

where M is the mass of the scalar field ϕ . Assuming the slow-roll conditions are satisfied, we can immediately obtain the two slow-roll equations (i.e., Eqs. (2.14)) as

$$H \simeq \frac{M}{2} \left(1 - e^{-\sqrt{2/3}\phi}\right), \quad \phi_N \simeq -2\sqrt{\frac{2}{3}} \frac{e^{-\sqrt{2/3}\phi}}{\left(1 - e^{-\sqrt{2/3}\phi}\right)}, \quad (3.12)$$

and the slow-roll parameters can be expressed in terms of the field ϕ as (i.e., Eqs. (2.15)):

$$\epsilon_1 \simeq \frac{4e^{-2\sqrt{2/3}\phi}}{3\left(1 - e^{-\sqrt{2/3}\phi}\right)^2}, \quad \epsilon_2 \simeq \frac{8e^{-\sqrt{2/3}\phi}}{3\left(1 - e^{-\sqrt{2/3}\phi}\right)^2}. \quad (3.13)$$

With the help of Eq. (3.12), one can easily solve the scalar field solution in terms of the e-folding number N_k , and the solutions of the slow-roll parameters at the leading order can be obtained as:

$$\epsilon_1 \simeq \frac{3}{4N_k^2}, \quad \epsilon_2 \simeq \frac{2}{N_k}, \quad (3.14)$$

and, using the leading order slow-roll approximation, i.e., Eqs. (2.16), we can quickly evaluate the scalar spectral index and the tensor-to-scalar ratio in terms of the e-folding number as:

$$n_s \simeq 1 - \frac{2}{N_k}, \quad r \simeq \frac{12}{N_k^2}. \quad (3.15)$$

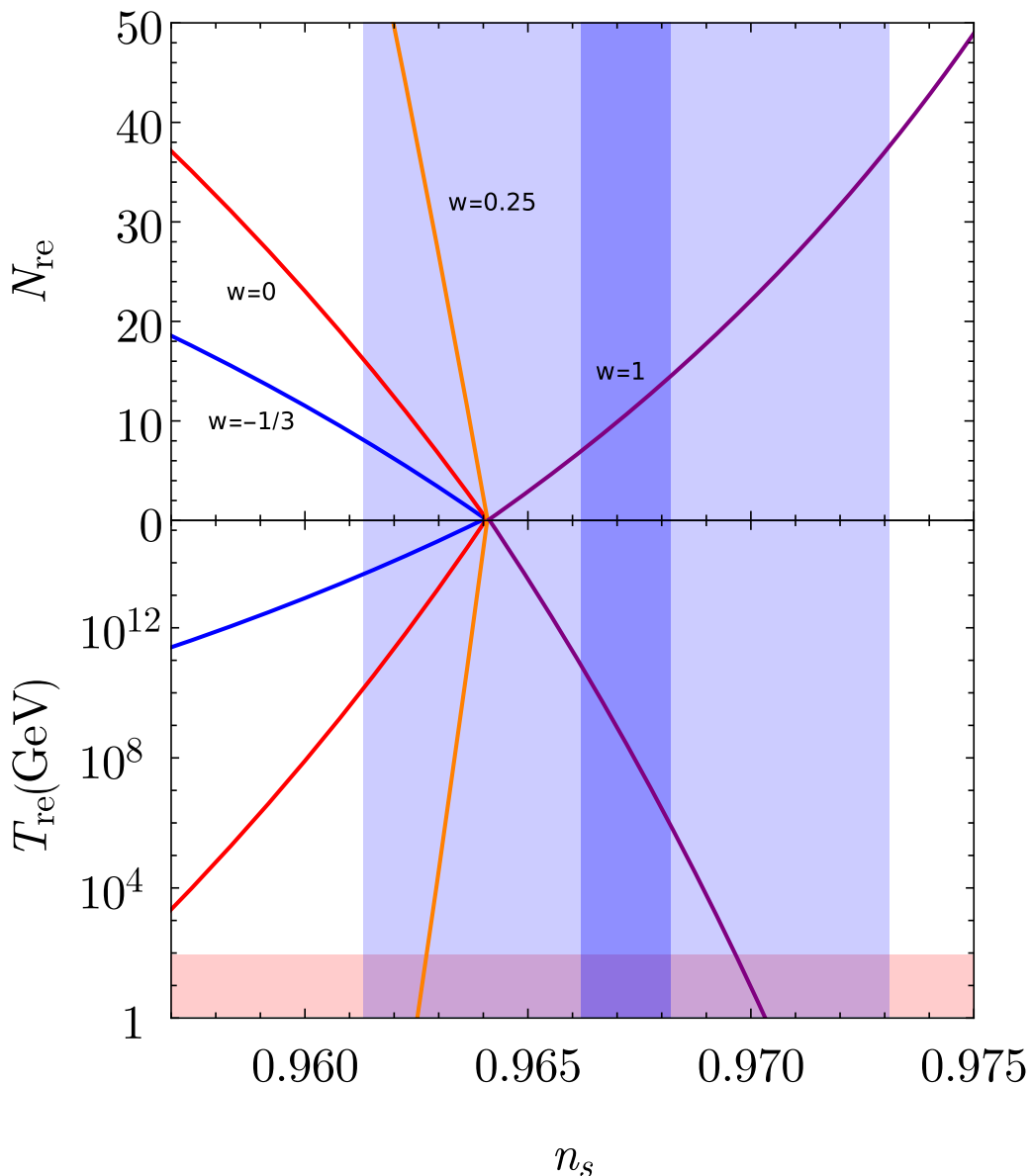


Figure 2: We plot the duration of reheating N_{re} and reheating temperature T_{re} given in Eqs. (3.8) and (3.9) as function of the scalar spectral index n_s given by Eq. (3.15) parametrically for the case of Starobinsky inflation. Please note that different colors represent dynamics corresponding to different effective EoS parameter w_{re} as indicated in the figure. The blue-shaded region represents the 1σ constraint on the value of n_s using ongoing observations [32–35] with $n_s = 0.9672 \pm 0.0059$. The dark blue region shows the future projected bound on n_s with a sensitivity of 10^{-3} , assuming its central value remains unchanged. The temperature below the lighter red region is excluded due to the constraint from the electroweak scale, which is taken to be 100 GeV.

Using the above equation along with Eqs. (3.8) and (3.9), one can obtain parametric dependence of N_{re} and T_{re} on n_s . In the case of the Starobinsky model, this is shown in

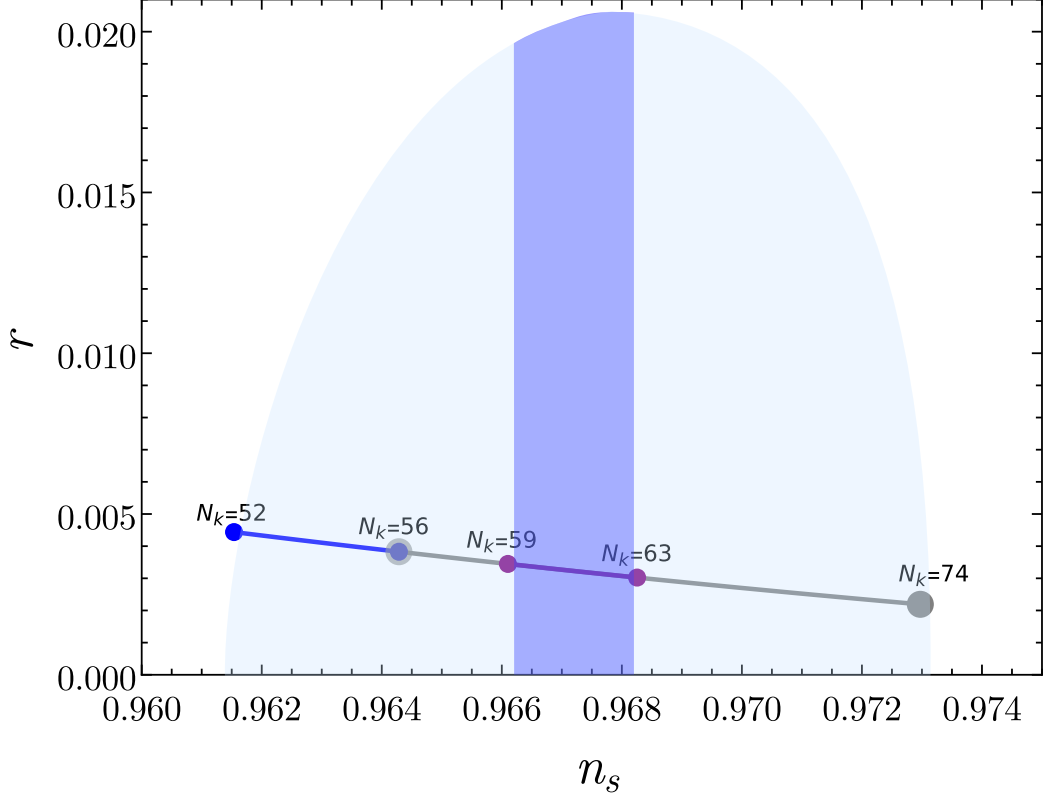


Figure 3: We plot the inflationary observables, tensor-to-scalar ratio (r) as a function of scalar spectral index (n_s) for the Starobinsky model using slow-roll approximations given by Eq. (3.15). This evolution is presented considering the bound on duration N_k using the reheating regime. We consider different EoS parameters during reheating w_{re} and observe the constraint on the duration N_k . Correspondingly, in the figure, blue line corresponds to the bound for $w_{\text{re}} < 1/3$, the gray line for $w_{\text{re}} > 1/3$ and the purple line for the future observational bound of n_s . The blue-shaded region represents the 1σ constraint on the value of n_s using ongoing observations [32–35] with $n_s = 0.9672 \pm 0.0059$. The dark blue region shows the future projected bound on n_s with a sensitivity of 10^{-3} , assuming its central value remains unchanged.

Fig. 2. Keep in mind that, $N_{\text{re}} \geq 0$, with $N_{\text{re}} \ll 1$ is referred to as instantaneous reheating [91, 92]. It immediately leads to the constraint on the value of n_s . For example, considering that during reheating, the evolution of the Universe effectively behaves as matter-expansion, i.e., $w_{\text{re}} = 0$. Thus, in the 1σ domain, we get the bound on N_k as

$$52 \leq N_k \leq 56 \quad (3.16)$$

and correspondingly, the bound on n_s becomes:

$$0.961 \leq n_s \leq 0.964 \quad (3.17)$$

In fact, as can be seen, for $w_{\text{re}} < 1/3$, it is obvious that there is an upper bound on N_k , which implies a bound on n_s as well, i.e., $N_k \leq 56$ and $n_s < 0.964$. It also immediately puts a tight constraint on N_{re} and T_{re} (for $w_{\text{re}} = 0$) as

$$N_{\text{re}} \leq 16, \quad T_{\text{re}} \geq 10^{10} \text{ GeV}. \quad (3.18)$$

However, during reheating, if we assume $w_{\text{re}} > 1/3$, these constraints flip and in the 1σ domain, there arises a new bound with a lower value of N_k as well as in n_s as

$$56 \leq N_k \leq 74, \quad 0.964 \leq n_s \leq 0.973. \quad (3.19)$$

Consequently, the bound on reheating parameters becomes (for $w_{\text{re}} = 1$)

$$N_{\text{re}} \leq 37, \quad T_{\text{re}} \geq 10^{-9} \text{ GeV}. \quad (3.20)$$

Considering these bounds into account, we plot r as a function of n_s in Fig. 3. Further, instead of looking in 1σ limit, if we consider the observational constraints proposed by the forthcoming experiments such as PRISM [93] and EUCLID [94], cosmic 21-cm surveys [66], and CORE experiments [67], which offer a precision enhancement of 10^{-3} in n_s , the constraints on N_k , N_{re} and T_{re} can be substantially improved¹. Then one can immediately refer from the Fig. 2 and 3 that for $w_{\text{re}} < 1/3$, the scalar spectral index does not satisfy the constraints in 1σ level posed by future observations. Therefore, under these conditions, this model can be ruled out. The model can be survived if one assumes $w_{\text{re}} > 1/3$, and the bound on N_{re} and T_{re} for the constraints posed by future observations becomes

$$7 \leq N_{\text{re}} \leq 14, \quad 10^9 \text{ GeV} \geq T_{\text{re}} \geq 10^6 \text{ GeV}. \quad (3.21)$$

Even in that case, if the future observations detect instantaneous reheating [91, 92], i.e., $N_{\text{re}} \ll 1$, n_s appears to be outside of the contour from the future observations. Therefore, unless $w > 1/3$ with the prolonged reheating era, the analytical approximation may lead to ruling out the Starobinsky inflation model. However, keeping aside the future observations, in the next section, we will see a significant improvement in these constraints by implementing meaningful corrections to the dynamics rather than the analytical approximations.

4 Numerical improvements

In the previous section, we discussed the CMB constraints on various inflationary models, which depend on the effective EoS parameter w_{re} as well as the duration of the reheating epoch N_{re} . There are two issues associated with this analysis. First, around and at the end of inflation, the slow-roll approximation breaks down. Yet, in evaluating duration N_k as well as energy density at end of inflation ρ_{end} in Eq. (3.8), we rely upon slow-roll approximations. Second, in evaluating perturbed observables in Eqs. (2.16), we consider only the leading-order contributions and ignore higher-order contributions, assuming their impact to be negligible. However, as anticipated in Refs. [71, 72], considering accurate dynamics rather than the slow-roll approximations may lead to notable enhancements in these predictions. Additionally, one can consider the onset of reheating not at the end of inflation but at the bottom of the potential, as will be discussed in the subsequent section. The implementation and, therefore, the resulting corrections due to these considerations can be categorized into three parts:

1. Implementation of accurate inflationary dynamics through numerical methods instead of slow-roll approximations.
2. Implementation of higher-order slow-roll approximations instead of leading-order slow-roll approximations.

¹The central value of n_s is assumed to be 0.9672 [35]

3. Implementation of onset of reheating as the bottom of the potential instead of the end of inflation.

In the following sections, we will conduct a detailed study of the impact of each of these corrections on the observational constraints. We will also compare the cumulative effects of these corrections with the existing predictions presented in the previous section.

4.1 Implementation of accurate inflationary dynamics through numerical methods

As mentioned earlier, this epoch of the slow-roll regime lasts as long as both of the slow-roll parameters are small, i.e., ($\epsilon_1 \ll 1$, $\epsilon_2 \ll 1$). On the other hand, $\epsilon_1 = 1$ signals the end of inflation. It turns out that even before the end of inflation, these slow approximations break down. Despite this, we still rely on (leading-order) slow-roll approximations even at the end of inflation to determine the analytical solution of the background variables, assuming the contribution due to accurate dynamics in evaluating perturbed observables is negligible. However, it is crucial, as in this section, we shall learn the significance of obtaining the accurate values of not only the background parameters but also the end of inflation. To illustrate this, let's now discuss this in detail with an example: the Starobinsky inflation.

Using leading-order slow-roll approximations and solving the slow-roll equations (*viz.* Eqs. (2.14)):

$$H^2 \simeq \frac{V}{3}, \quad \phi_N \simeq -\frac{V_\phi}{V},$$

with the initial condition $\phi_i = 5.8$, we obtain the following results:

$$N_{\text{end}} \simeq 80.86, \quad \phi_{\text{end}} \simeq 0.94, \quad H_{\text{end}} \simeq 0.267 M, \quad \rho_{\text{end}} \simeq 0.215 M^2,$$

along with the slow-roll solutions given in Eqs. (3.14). Here, N_{end} is the duration of the field rolling from the initial value ϕ_i to ϕ_{end} , i.e., the duration of inflation. These values are essential for the analysis in Eqs. (3.8) and (3.9) which has been shown in the previous section with Fig. 2.

To improve the analysis, in this section, we now consider, rather than the slow-roll, the full inflationary equations (*viz.* Eqs. (2.9) and (2.10)):

$$H = \sqrt{\frac{V}{3 - \frac{1}{2}\phi_N^2}}, \quad \phi_{NN} + \left(3 - \frac{1}{2}\phi_N^2\right) \left(\phi_N + \frac{V_\phi}{V}\right) = 0.$$

Solving the highly non-linear differential equation with identical initial condition $\phi_i = 5.8$, we now obtain the numerical solutions of the background variables such as the Hubble parameter and the slow-roll parameters along with:

$$N_{\text{end}} \simeq 82.48, \quad \phi_{\text{end}} \simeq 0.61, \quad H_{\text{end}} = 0.241 M, \quad \rho_{\text{end}} \simeq 0.175 M^2.$$

Thus, there is a significant improvement not only in the numerical solution of the background variables but also in H_{end} , ρ_{end} , and N_{end} . These improvements directly impact the reheating analysis in two ways. The first is the direct influence of ρ_{end} in Eq. (3.8). The second, and more crucial, impact is the significant improvement in $\Delta N_{\text{end}} = \Delta N_k \sim 1.5$, which in turn enhances the accuracy of the background variables. For example, in the case of leading order approximations, $\{\epsilon_1, \epsilon_2\} \simeq \{0.0003, 0.040\}$ for $N_k = 50$, whereas, numerically we obtain

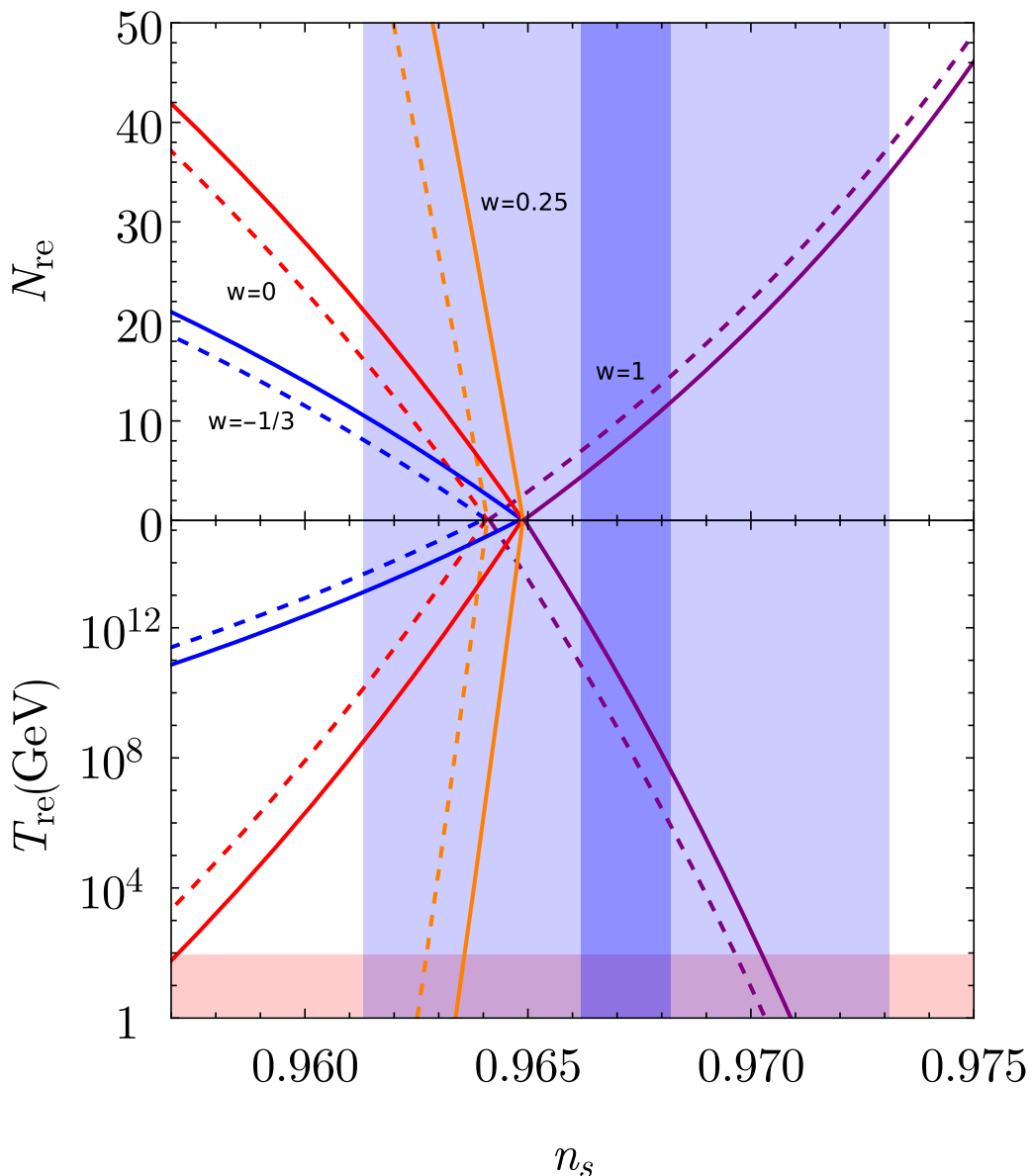


Figure 4: We plot the duration of reheating N_{re} and reheating temperature T_{re} given by Eqs. (3.8) and (3.9) as function of the scalar spectral index n_s parametrically for both analytical and numerical solution, given by Eqs. (3.15), (2.16) respectively. The solid lines are for the numerical solution, and the dashed lines are for the analytically approximated solution. Please note that different colors represent dynamics corresponding to different effective equations of state parameter w_{re} as indicated in the figure. The blue-shaded region represents the 1σ constraint on the value of n_s using ongoing observations [32–35] with $n_s = 0.9672 \pm 0.0059$. The dark blue region shows the future projected bound on n_s with a sensitivity of 10^{-3} , assuming its central value remains unchanged. The temperature below the lighter red region is excluded due to the constraint from the electroweak scale, which is taken to be 100 GeV.

these values as $\{\epsilon_1, \epsilon_2\} \simeq \{0.00027, 0.038\}$, and thus $\Delta n_s \simeq 2 \times 10^{-3}$, as also discussed in Ref. [71]².

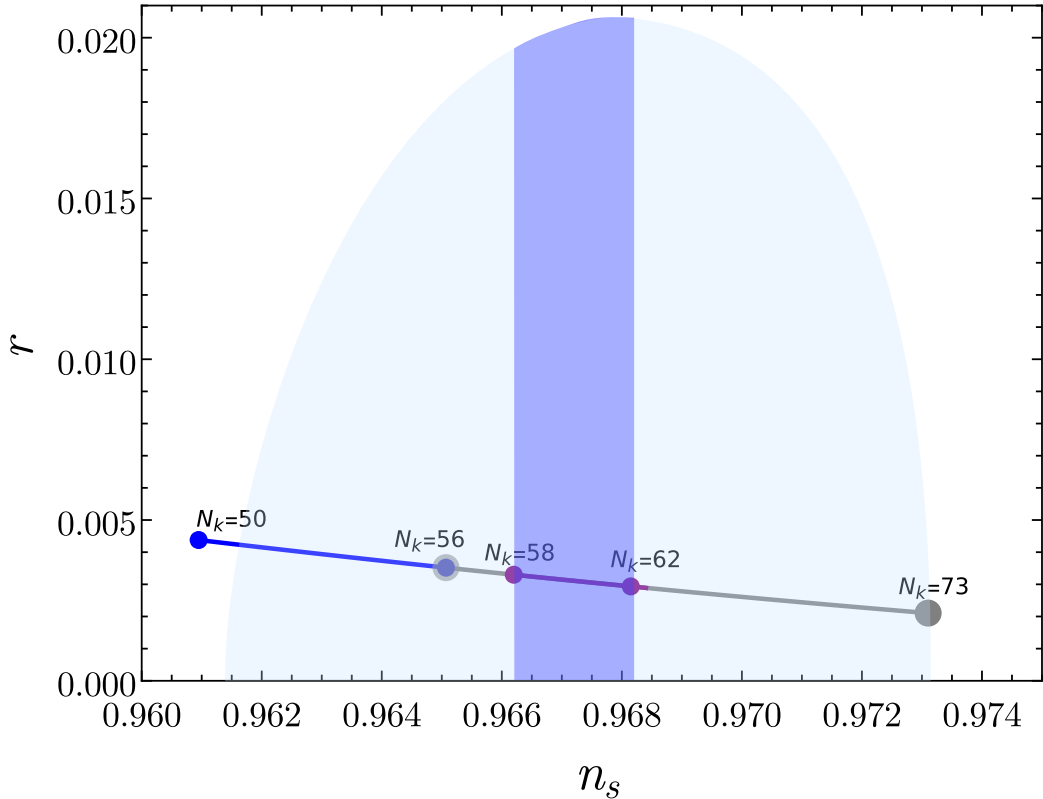


Figure 5: We plot the inflationary observables, tensor-to-scalar ratio (r) as a function of scalar spectral index (n_s) for the Starobinsky model using numerical solution given by Eq. (2.16). This evolution is presented considering the bound on duration N_k using the reheating regime. We consider different EoS parameters during reheating w_{re} and observe the constraint on the duration N_k . Correspondingly, in the figure, blue line corresponds to the bound for $w_{\text{re}} < 1/3$, the gray line for $w_{\text{re}} > 1/3$ and the purple line for the future observational bound of n_s . The blue-shaded region represents the 1σ constraint on the value of n_s using ongoing observations [32–35] with $n_s = 0.9672 \pm 0.0059$. The dark blue region shows the future projected bound on n_s with a sensitivity of 10^{-3} , assuming its central value remains unchanged.

We now examine the impact of this on the reheating analysis and compare the results with the results obtained using slow-roll approximations. This is illustrated in Fig. 4. As anticipated, the improvement is significant. In the figure, one can see that numerical predictions show a significant shift to the right in the estimates of N_{re} and T_{re} . Due to this shift, the bound on N_k , and subsequently n_s also changes, with an improvement being $\Delta n_s \sim 10^{-3}$. For example, in the case of leading-order slow-roll approximation with $w_{\text{re}} < 1/3$, the upper bound on n_s is: $n_s \leq 0.964$, whereas, in this improved case, the bound becomes $n_s \leq 0.965$. The improvements are explicitly shown in the Table 1. This confirms

²Please note that, for a multi-parameter model, numerical evaluation for the entire range of the parameters can be challenging. In that case, one can rely upon a semi-analytical solution presented in Ref. [71], where analytically obtained solutions are nearly comparable to the numerical solutions.

	Analytical approximations	Numerical solution
$w_{\text{re}} < 1/3$	$52 \leq N_k \leq 56,$ $0.9613 \leq n_s \leq 0.9641$ $N_{\text{re}} \leq 16 (w_{\text{re}} = 0),$ $T_{\text{re}} \geq 10^{10} \text{ GeV} (w_{\text{re}} = 0)$	$50 \leq N_k \leq 56,$ $0.9613 \leq n_s \leq 0.9649,$ $N_{\text{re}} \leq 21 (w_{\text{re}} = 0),$ $T_{\text{re}} \geq 10^8 \text{ GeV} (w_{\text{re}} = 0)$
$w_{\text{re}} > 1/3$	$56 \leq N_k \leq 74,$ $0.9641 \leq n_s \leq 0.9731,$ $N_{\text{re}} \leq 37 (w_{\text{re}} = 1),$ $T_{\text{re}} \geq 10^{-9} \text{ GeV} (w_{\text{re}} = 1)$	$56 \leq N_k \leq 73,$ $0.9649 \leq n_s \leq 0.9731,$ $N_{\text{re}} \leq 34 (w_{\text{re}} = 1),$ $T_{\text{re}} \geq 10^{-8} \text{ GeV} (w_{\text{re}} = 1)$
future observations ($w_{\text{re}} > 1/3$: allowed) ($w_{\text{re}} < 1/3$: not allowed)	$59 \leq N_k \leq 63,$ $0.9662 \leq n_s \leq 0.9682,$ $7 \leq N_{\text{re}} \leq 14 (w_{\text{re}} = 1),$ $10^9 \text{ GeV} \geq T_{\text{re}} \geq 10^6 \text{ GeV} (w_{\text{re}} = 1)$	$58 \leq N_k \leq 62,$ $0.9662 \leq n_s \leq 0.9682,$ $4 \leq N_{\text{re}} \leq 12 (w_{\text{re}} = 1),$ $10^{12} \text{ GeV} \geq T_{\text{re}} \geq 10^7 \text{ GeV} (w_{\text{re}} = 1)$

Table 1: Starobinsky Inflation: The bounds on variables, N_k , n_s , N_{re} , and T_{re} for different values of w_{re} corresponding to analytically (slow-roll) approximated and the numerical solutions.

our anticipation that the accurate dynamics help improve the theoretical predictions, which is one of the main results of this work.

4.2 Implementation of higher-order slow-roll approximations

In the previous section, we estimated the reheating parameters and e-folding number using the numerical background solution with the leading order inflationary observables, i.e., Eqs. (2.16). However, as mentioned earlier, these expressions are obtained using leading-order slow-roll, and the full solutions of the amplitude of scalar power spectrum, scalar spectral index as well as the tensor-to-scalar ratio in terms of the slow-roll parameter are given as [25, 73]:

$$\begin{aligned}
A_s = & 1 - 2(C + 1)\epsilon_1 - C\epsilon_2 + \left(2C^2 + 2C + \frac{\pi^2}{2} - f\right)\epsilon_1^2 + \left(C^2 - C + \frac{7\pi^2}{12} - g\right)\epsilon_1\epsilon_2 \\
& + \left(\frac{1}{2}C^2 + \frac{\pi^2}{8} - 1\right)\epsilon_2^2 + \left(-\frac{1}{2}C^2 + \frac{\pi^2}{24}\right)\epsilon_2\epsilon_3,
\end{aligned} \tag{4.1}$$

$$n_s = 1 - 2\epsilon_1 - \epsilon_2 - 2\epsilon_1^2 - (3 + 2C)\epsilon_1\epsilon_2 - C\epsilon_2\epsilon_3, \tag{4.2}$$

$$r = 16\epsilon_1\left(1 + 2C\frac{\epsilon_2}{2}\right), \tag{4.3}$$

where $C = -2 + \ln 2 + \gamma$, where γ is the Euler constant, $f = 5$ and $g = 7$. In this section, instead of using Eqs. (2.16), along with the numerical solution, we consider the above expressions for the observable, repeat the reheating analysis, and compare our results with

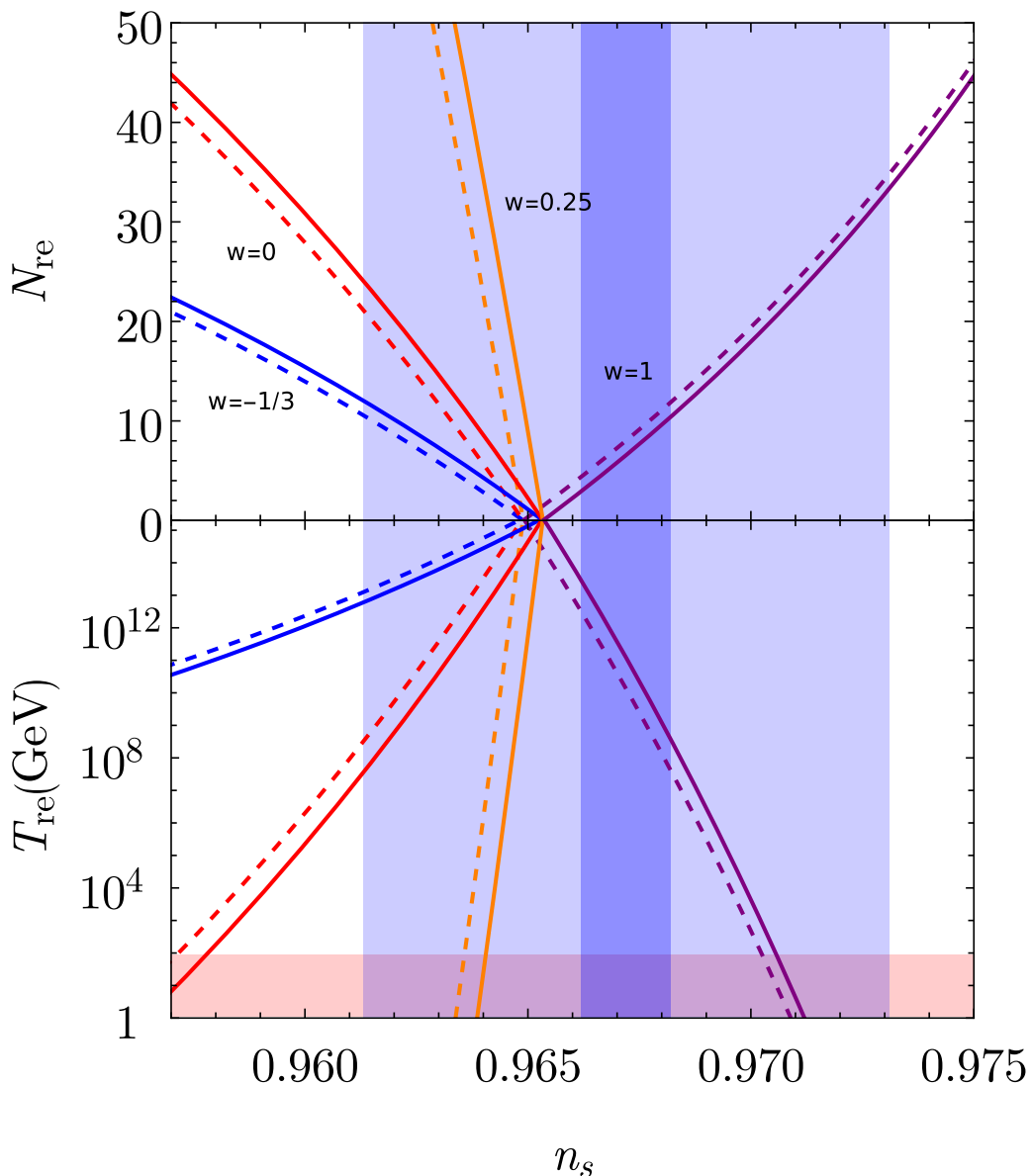


Figure 6: We plot the duration of reheating N_{re} and reheating temperature T_{re} given by Eqs. (3.8) and (3.9) as function of the scalar spectral index n_s parametrically comparing numerical solution with leading-order approximations and numerical solution with higher-order approximations given by Eq. (2.16), (4.2) respectively. The solid lines are for the higher-order approximations and the dashed lines are for the leading-order approximations. Please note that different colors represent dynamics corresponding to different effective equations of state parameter w_{re} as indicated in the figure. The blue-shaded region represents the 1σ constraint on the value of n_s using ongoing observations[32–35] with $n_s = 0.9672 \pm 0.0059$. The dark blue region shows the future projected bound on n_s with a sensitivity of 10^{-3} , assuming its central value remains unchanged. The temperature below the lighter red region is excluded due to the constraint from the electroweak scale, which is taken to be 100 GeV.

the numerical results obtained in the previous section, which has been illustrated in Figs. 6 and 7 as well as in Table 2.

As again can be seen in Fig. 6, there is a further shift in reheating parameters, N_{re} and T_{re} compared to the improvements mentioned in the previous section. We obtain an additional improvement of $\Delta n_s \sim 4 \times 10^{-4}$, resulting a new bound on n_s becomes $n_s \leq 0.9653$ for $w_{\text{re}} < 1/3$. Thus, considering higher-order slow-roll approximations instead of the leading-order can significantly improve the estimation of the observables by an order of $\sim 10^{-3}$. The detailed bounds on parameters are shown in the Table 2.

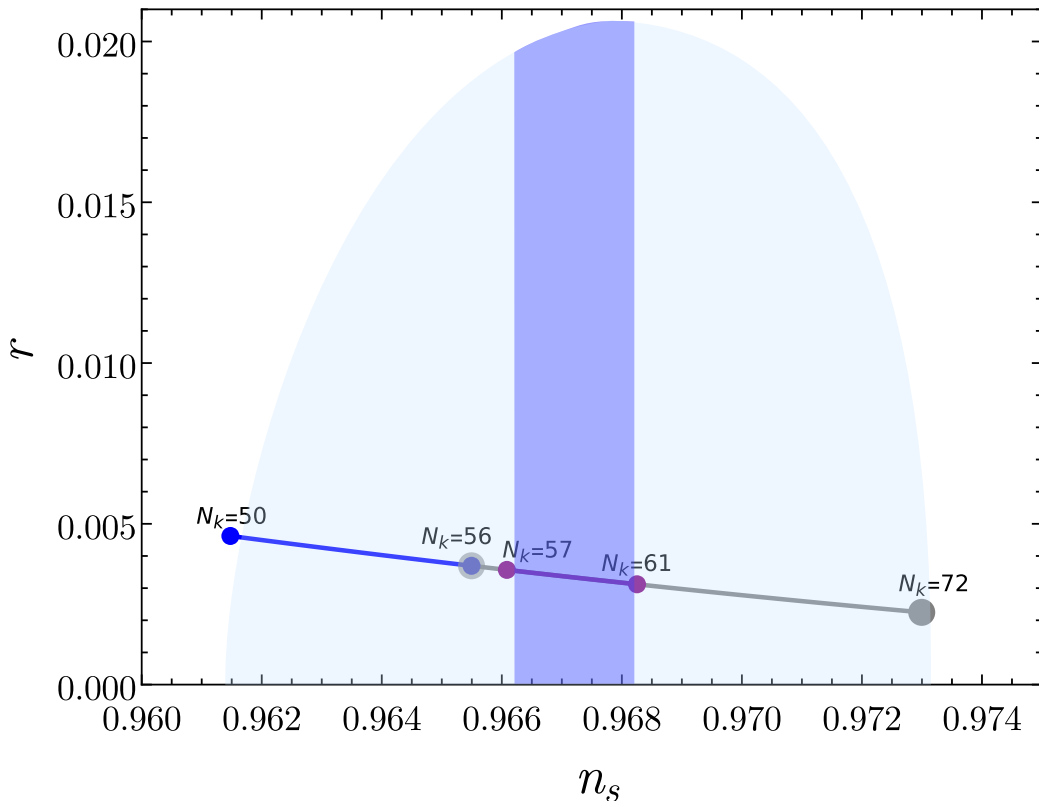


Figure 7: We plot the inflationary observables, tensor-to-scalar ratio (r) as a function of scalar spectral index (n_s) for the Starobinsky model using higher-order approximations given by Eq. (4.2), (4.3). This evolution is presented considering the bound on duration N_k using the reheating regime. We consider different EoS parameters during reheating w_{re} and observe the constraint on the duration N_k . Correspondingly, in the figure, blue line corresponds to the bound for $w_{\text{re}} < 1/3$, the gray line for $w_{\text{re}} > 1/3$ and the purple line for the future observational bound of n_s . The blue-shaded region represents the 1σ constraint on the value of n_s using ongoing observations [32–35] with $n_s = 0.9672 \pm 0.0059$. The dark blue region shows the future projected bound on n_s with a sensitivity of 10^{-3} , assuming its central value remains unchanged.

	Numerical solution with leading-order n_s, r expressions	Numerical solution with higher-order n_s, r expressions
$w_{\text{re}} < 1/3$	$50 \leq N_k \leq 56,$ $0.9613 \leq n_s \leq 0.9649$ $N_{\text{re}} \leq 21(w_{\text{re}} = 0),$ $T_{\text{re}} \geq 10^8 \text{ GeV}(w_{\text{re}} = 0)$	$50 \leq N_k \leq 56,$ $0.9613 \leq n_s \leq 0.9653,$ $N_{\text{re}} \leq 24(w_{\text{re}} = 0),$ $T_{\text{re}} \geq 10^7 \text{ GeV}(w_{\text{re}} = 0)$
$w_{\text{re}} > 1/3$	$56 \leq N_k \leq 73,$ $0.9649 \leq n_s \leq 0.9731,$ $N_{\text{re}} \leq 34(w_{\text{re}} = 1),$ $T_{\text{re}} \geq 10^{-8} \text{ GeV}(w_{\text{re}} = 1)$	$56 \leq N_k \leq 72,$ $0.9653 \leq n_s \leq 0.9731,$ $N_{\text{re}} \leq 33(w_{\text{re}} = 1),$ $T_{\text{re}} \geq 10^{-7} \text{ GeV}(w_{\text{re}} = 1)$
future observations ($w_{\text{re}} > 1/3$: allowed) ($w_{\text{re}} < 1/3$: not allowed)	$58 \leq N_k \leq 62,$ $0.9662 \leq n_s \leq 0.9682,$ $4 \leq N_{\text{re}} \leq 12(w_{\text{re}} = 1),$ $10^{12} \text{ GeV} \geq T_{\text{re}} \geq 10^7 \text{ GeV}(w_{\text{re}} = 1)$	$57 \leq N_k \leq 61,$ $0.9662 \leq n_s \leq 0.9682,$ $3 \leq N_{\text{re}} \leq 10(w_{\text{re}} = 1),$ $10^{13} \text{ GeV} \geq T_{\text{re}} \geq 10^8 \text{ GeV}(w_{\text{re}} = 1)$

Table 2: Starobinsky Inflation: The bounds on variables, N_k , n_s , N_{re} , and T_{re} for different values of w_{re} corresponding to leading-order approximations and the higher-order approximations. Note that, in both cases, the background solutions are numerically obtained.

4.3 Implementation of the onset of reheating as the bottom of the potential

Till now, we were estimating N_{re} and T_{re} , considering the onset of the reheating era after the end of inflation. However, in Ref. [62], it has been shown that, instead of considering minimal gravity theory, if one considers modified gravity theories, the onset of reheating as the end of inflation can make a significant change in the analysis. This is because, ϵ_1 is not a invariant under conformal transformation. Therefore, in a meaningful manner, one can choose the onset of reheating as the bottom of the potential, as this point is conformally invariant, and can be used even for general modified gravity theories. Therefore, in this section, we introduce corrections to the reheating analysis, and thus the observables, by considering that the reheating era commences after the epoch at which the potential touches its minima (bottom of the potential). In that case, Eq. (3.8) can be re-written as

$$N_{\text{re}} = \frac{4}{1-3w_{\text{re}}} \left(-N_k - N_{\text{eb}} - \frac{1}{4} \log \left(\frac{30}{\pi^2 g_{\text{reh}}} \right) - \frac{1}{3} \log \left(\frac{11g_{\text{s, re}}}{43} \right) - \log \left(\frac{k}{a_0 T_0} \right) - \frac{1}{4} \log \rho_b + \log H_k \right), \quad (4.4)$$

and the reheating temperature, i.e., Eq. (3.9) can also be evaluated as:

$$T_{\text{re}} = \frac{a_0 T_0}{k} \left(\frac{43}{11g_{\text{s, re}}} \right) e^{-N_k - N_{\text{eb}} - N_{\text{re}}}. \quad (4.5)$$

Here, $N_{\text{eb}} \equiv a_b/a_{\text{end}}$ and $\rho_b \equiv 3H_b^2$, where (b) denotes the bottom of the potential. Again, we perform our analysis considering the numerically obtained solution with higher-order slow-

roll corrections and the onset of reheating as the bottom of the potential. However, to our surprise, we find that this implementation does not improve the accuracy to a significant amount, as $\Delta n_s \sim 10^{-5}$.

To summarize our cumulative result, in Fig. 8, we plot the results obtained through the analytical approximations mentioned in the first section and the improvement obtained through the implementation of three corrections to the dynamics, and Table 3 summarizes all the results. Compared to the conventional analytical case, our corrections improve the accuracy in n_s to $\Delta n_s \sim 1.2 \times 10^{-3}$, which is significant. Note that, if the central value of n_s is assumed to be ~ 0.9672 even in this case, then even with the improvements, the Starobinsky model can indeed be ruled out at 1σ level from the expected future observation. These are the main results of this work.

	Analytical approximations	Higher-order approximations
$w_{\text{re}} < 1/3$	$52 \leq N_k \leq 56,$ $0.9613 \leq n_s \leq 0.9641,$ $N_{\text{re}} \leq 16 (w_{\text{re}} = 0),$ $T_{\text{re}} \geq 10^{10} \text{ GeV} (w_{\text{re}} = 0)$	$50 \leq N_k \leq 56,$ $0.9613 \leq n_s \leq 0.9653,$ $N_{\text{re}} \leq 24 (w_{\text{re}} = 0),$ $T_{\text{re}} \geq 10^7 \text{ GeV} (w_{\text{re}} = 0)$
$w_{\text{re}} > 1/3$	$56 \leq N_k \leq 74,$ $0.9641 \leq n_s \leq 0.9731,$ $N_{\text{re}} \leq 37 (w_{\text{re}} = 1),$ $T_{\text{re}} \geq 10^{-9} \text{ GeV} (w_{\text{re}} = 1)$	$56 \leq N_k \leq 72,$ $0.9653 \leq n_s \leq 0.9731,$ $N_{\text{re}} \leq 33 (w_{\text{re}} = 1),$ $T_{\text{re}} \geq 10^{-7} \text{ GeV} (w_{\text{re}} = 1)$
future observations ($w_{\text{re}} > 1/3$: allowed) ($w_{\text{re}} < 1/3$: not allowed)	$59 \leq N_k \leq 63,$ $0.9662 \leq n_s \leq 0.9682,$ $7 \leq N_{\text{re}} \leq 14 (w_{\text{re}} = 1),$ $10^9 \text{ GeV} \geq T_{\text{re}} \geq 10^6 \text{ GeV} (w_{\text{re}} = 1)$	$57 \leq N_k \leq 61,$ $0.9662 \leq n_s \leq 0.9682,$ $3 \leq N_{\text{re}} \leq 10 (w_{\text{re}} = 1),$ $10^{13} \text{ GeV} \geq T_{\text{re}} \geq 10^8 \text{ GeV} (w_{\text{re}} = 1)$

Table 3: Starobinsky Inflation: The bounds on variables, N_k , n_s , N_{re} , and T_{re} for different values of w_{re} corresponding to analytical approximated parameters, and numerical solution with higher-order approximations.

5 Summary and conclusions

In this article, we consider a single canonical scalar field model minimally coupled to the gravity with a potential $V(\phi)$ that drives the evolution of the early Universe, including both slow-roll inflation and oscillatory solution around the minima of the potential, also known as the reheating epoch. In obtaining the solution, we often use different sets of approximations in both regimes. In the slow-roll inflationary regime, where $\epsilon_1, \epsilon_2 \ll 1$, we rely upon the slow-roll approximations. In contrast, the reheating epoch is, for simplicity, quantitatively characterized by the effective EoS parameter w_{re} and the duration of this epoch N_{re} (or

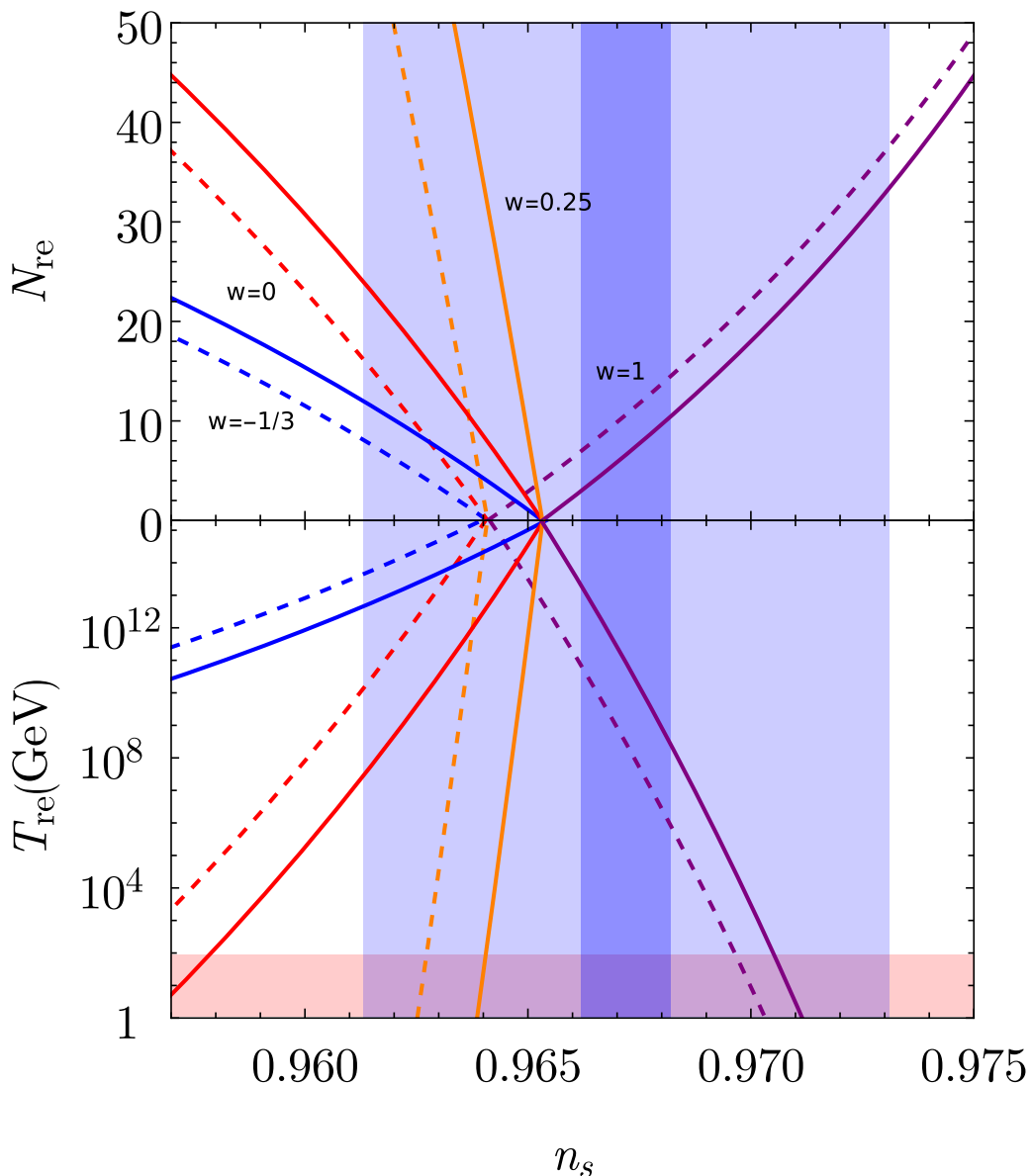


Figure 8: We plot the duration of reheating N_{re} and reheating temperature T_{re} given by Eqs. (3.8) and (3.9) as function of the scalar spectral index n_s parametrically comparing analytically approximated solution and numerical solution with higher-order approximations, given by Eqs. (3.15), (4.2) respectively. The solid lines are for the onset of reheating as the bottom of the potential and the dashed lines are for the analytically approximated solution. Please note that different colors represent dynamics corresponding to different effective equations of state parameter w_{re} as indicated in the figure. The blue-shaded region represents the 1σ constraint on the value of n_s using ongoing observations [32–35] with $n_s = 0.9672 \pm 0.0059$. The dark blue region shows the future projected bound on n_s with a sensitivity of 10^{-3} , assuming its central value remains unchanged. The temperature below the lighter red region is excluded due to the constraint from the electroweak scale, which is taken to be 100 GeV.

the reheating temperature T_{re}). However, these approximations may lead to a significant discrepancy in the theoretical estimation of the observables (n_s and r). While accurately defining the reheating epoch (*viz.* the qualitative analysis) is challenging, this work focuses on examining the impact of a more accurate dynamics, rather than the slow-roll approximations, on the perturbed observables.

In order to do this, we specifically considered the following improvements in the dynamics:

1. Numerical Solution: In this method, we solve the complete background Eq. (2.10) using the numerical method, which provides us with an accurate solution for the dynamics of the Universe in its early phase. Using this solution, we estimate the observables and compare the results with the solutions obtained using slow roll approximation.
2. Higher-order approximations: This method includes higher-order slow-roll corrections to the inflationary observables, Eqs. (4.1), (4.2) and (4.3), rather than Eqs. (2.16). Here also, we used complete numerical solution and estimated the observables using higher order slow-roll corrections and estimated the discrepancy in the observables with respect to the analytical solution obtained using slow-roll approximation.
3. Onset of the reheating as the bottom of the potential: Typically, the end of inflation is considered the onset of the reheating epoch. However, in this method, we show that if reheating begins at the bottom of the potential, the reheating parameters are modified, as given by Eq. (4.4) and Eq. (4.5). This modification can provide a new bound on the duration N_k , leading to a discrepancy in the scalar spectral index.

After implementing these changes, we found an improvement in the theoretical bounds on the observables. As seen in Fig. 8, there is an improvement of $\Delta n_s \sim 1.2 \times 10^{-3}$. These numerical predictions indicate that for $w_{\text{re}} < 1/3$, the Starobinsky model has an upper bound as $n_s \leq 0.9653$. This can be ruled out from the future observational constraint if the central value is $n_s \simeq 0.9672$ [35]. However, for $w_{\text{re}} > 1/3$, the reheating parameters fall within the future observational bounds, though, at the cost of sufficient reheating e-folding number ($\sim \mathcal{O}(1-2)$). This scenario can again be ruled out if future observations detect instantaneous reheating [91, 92].

The result is compelling, as now it has been established that corrections due to accurate dynamics or higher-order slow-roll approximations can not be ignored. This also implies that even seemingly minor corrections must be considered and implemented to study their implications on perturbed observables. Therefore, when obtaining observational bounds on any inflationary models, one must consider all these corrections, which have been reserved for future endeavors.

In addition to these methods, other improvements can also be made to further enhance the accuracy. For example, in this work, we only considered the slow-roll dynamics, but one could also improve the reheating analysis by incorporating qualitative analysis of the reheating and implementing the changes into the quantitative analysis. Second, higher-order correlation such as non-Gaussianity (see, for instance, Refs. [95–99]) can play a pivotal role in the observables. Third, the implications of primordial black holes and primordial gravitational waves may also play a crucial role in inflationary and post-inflationary dynamics. Fourth, exploring the non-minimal sector instead of the minimal theory of gravity is another avenue. In fact, in our work, while the corrections due to the onset of reheating as the

bottom of the potential did not play a significant role, they could be significant in the non-minimal sector [62, 100]. Finally, extending the analysis to non-inflationary dynamics, such as viable classical bounces, is also possible. Recent studies [99, 101–107] show that these alternatives can also fit observations well. Therefore, one must consider all alternatives to slow-roll inflation and carefully study the analysis with all effects, even those that seem minor, to determine the observable constraints of the model.

References

- [1] A. A. Starobinsky, *Spectrum of relict gravitational radiation and the early state of the universe*, *JETP Lett.* **30** (1979) 682–685.
- [2] A. A. Starobinsky, *A New Type of Isotropic Cosmological Models Without Singularity*, *Phys. Lett. B* **91** (1980) 99–102.
- [3] A. H. Guth, *Inflationary universe: A possible solution to the horizon and flatness problems*, *Phys. Rev. D* **23** (Jan, 1981) 347–356.
- [4] K. Sato, *First-order phase transition of a vacuum and the expansion of the Universe*, *Monthly Notices of the Royal Astronomical Society* **195** (07, 1981) 467–479, [<http://oup.prod.sis.lan/mnras/article-pdf/195/3/467/4065201/mnras195-0467.pdf>].
- [5] V. F. Mukhanov and G. V. Chibisov, *Quantum Fluctuations and a Nonsingular Universe*, *JETP Lett.* **33** (1981) 532–535. [*Pisma Zh. Eksp. Teor. Fiz.*33,549(1981)].
- [6] A. Linde, *A new inflationary universe scenario: A possible solution of the horizon, flatness, homogeneity, isotropy and primordial monopole problems*, *Physics Letters B* **108** (1982), no. 6 389 – 393.
- [7] S. Hawking, *The development of irregularities in a single bubble inflationary universe*, *Physics Letters B* **115** (1982), no. 4 295 – 297.
- [8] A. A. Starobinsky, *Dynamics of Phase Transition in the New Inflationary Universe Scenario and Generation of Perturbations*, *Phys. Lett. B* **117** (1982) 175–178.
- [9] A. H. Guth and S.-Y. Pi, *Fluctuations in the new inflationary universe*, *Phys. Rev. Lett.* **49** (Oct, 1982) 1110–1113.
- [10] M. Sasaki, *Large Scale Quantum Fluctuations in the Inflationary Universe*, *Progress of Theoretical Physics* **76** (1986) 1036–1046.
- [11] A. Albrecht and P. J. Steinhardt, *Cosmology for grand unified theories with radiatively induced symmetry breaking*, *Phys. Rev. Lett.* **48** (Apr, 1982) 1220–1223.
- [12] A. D. Linde, *Chaotic Inflation*, *Phys. Lett.* **129B** (1983) 177–181.
- [13] A. Vilenkin, *Quantum fluctuations in the new inflationary universe*, *Nuclear Physics B* **226** (1983), no. 2 527 – 546.
- [14] J. M. Bardeen, P. J. Steinhardt, and M. S. Turner, *Spontaneous creation of almost scale-free density perturbations in an inflationary universe*, *Phys. Rev. D* **28** (Aug, 1983) 679–693.
- [15] E. W. Kolb and M. Turner, *The early universe*. Reading, Mass. : Addison-Wesley, May, 1990.
- [16] V. F. Mukhanov, H. A. Feldman, and R. H. Brandenberger, *Theory of cosmological perturbations. Part 1. Classical perturbations. Part 2. Quantum theory of perturbations. Part 3. Extensions*, *Phys. Rept.* **215** (1992) 203–333.
- [17] A. R. Liddle, P. Parsons, and J. D. Barrow, *Formalizing the slow roll approximation in inflation*, *Phys. Rev. D* **50** (1994) 7222–7232, [[astro-ph/9408015](https://arxiv.org/abs/astro-ph/9408015)].
- [18] J. E. Lidsey, A. R. Liddle, E. W. Kolb, E. J. Copeland, T. Barreiro, *et. al.*, *Reconstructing the inflation potential : An overview*, *Rev.Mod.Phys.* **69** (1997) 373–410, [[astro-ph/9508078](https://arxiv.org/abs/astro-ph/9508078)].

- [19] E. J. Copeland, A. R. Liddle, and D. Wands, *Exponential potentials and cosmological scaling solutions*, *Phys. Rev. D* **57** (1998) 4686–4690, [[gr-qc/9711068](#)].
- [20] J. Martin and R. H. Brandenberger, *The TransPlanckian problem of inflationary cosmology*, *Phys. Rev. D* **63** (2001) 123501, [[hep-th/0005209](#)].
- [21] A. Linde, *Particle Physics and Inflationary Cosmology*, *arXiv e-prints* (Mar., 2005) hep-th/0503203, [[hep-th/0503203](#)].
- [22] D. H. Lyth, *Particle physics models of inflation*, *Lect. Notes Phys.* **738** (2008) 81–118, [[hep-th/0702128](#)].
- [23] L. Sriramkumar, *An introduction to inflation and cosmological perturbation theory*, [arXiv:0904.4584](#).
- [24] D. Baumann, *Inflation*, in *Physics of the large and the small, TASI 09, proceedings of the Theoretical Advanced Study Institute in Elementary Particle Physics, Boulder, Colorado, USA, 1-26 June 2009*, pp. 523–686, 2011. [arXiv:0907.5424](#).
- [25] J. Martin, C. Ringeval, and V. Vennin, *Encyclopædia Inflationaris*, *Phys. Dark Univ.* **5-6** (2014) 75–235, [[arXiv:1303.3787](#)].
- [26] A. Linde, *Inflationary Cosmology after Planck 2013*, in *Proceedings, 100th Les Houches Summer School: Post-Planck Cosmology: Les Houches, France, July 8 - August 2, 2013*, pp. 231–316, 2015. [arXiv:1402.0526](#).
- [27] J. Martin, *The Observational Status of Cosmic Inflation after Planck*, *Astrophys. Space Sci. Proc.* **45** (2016) 41–134, [[arXiv:1502.0573](#)].
- [28] **Planck** Collaboration, P. Ade *et. al.*, *Planck 2015 results. XX. Constraints on inflation*, *Astron. Astrophys.* **594** (2016) A20, [[arXiv:1502.0211](#)].
- [29] **Planck** Collaboration, P. Ade *et. al.*, *Planck 2015 results. XVII. Constraints on primordial non-Gaussianity*, *Astron. Astrophys.* **594** (2016) A17, [[arXiv:1502.0159](#)].
- [30] S. Clesse, *An introduction to inflation after Planck: from theory to observations*, in *10th Modave Summer School in Mathematical Physics*, 1, 2015. [arXiv:1501.0046](#).
- [31] S. D. Odintsov, V. K. Oikonomou, I. Giannakoudi, F. P. Fronimos, and E. C. Lympieriadou, *Recent Advances in Inflation, Symmetry* **15** (2023), no. 9 1701, [[arXiv:2307.1630](#)].
- [32] **Planck** Collaboration, Y. Akrami *et. al.*, *Planck 2018 results. X. Constraints on inflation*, *Astron. Astrophys.* **641** (2020) A10, [[arXiv:1807.0621](#)].
- [33] **Planck** Collaboration, N. Aghanim *et. al.*, *Planck 2018 results. VI. Cosmological parameters*, *Astron. Astrophys.* **641** (2020) A6, [[arXiv:1807.0620](#)]. [Erratum: *Astron. Astrophys.* 652, C4 (2021)].
- [34] **BICEP, Keck** Collaboration, P. A. R. Ade *et. al.*, *Improved Constraints on Primordial Gravitational Waves using Planck, WMAP, and BICEP/Keck Observations through the 2018 Observing Season*, *Phys. Rev. Lett.* **127** (2021), no. 15 151301, [[arXiv:2110.0048](#)].
- [35] G. Galloni, N. Bartolo, S. Matarrese, M. Migliaccio, A. Ricciardone, and N. Vittorio, *Updated constraints on amplitude and tilt of the tensor primordial spectrum*, *JCAP* **04** (2023) 062, [[arXiv:2208.0018](#)].
- [36] A. Albrecht, P. J. Steinhardt, M. S. Turner, and F. Wilczek, *Reheating an Inflationary Universe*, *Phys. Rev. Lett.* **48** (1982) 1437.
- [37] L. F. Abbott, E. Farhi, and M. B. Wise, *Particle Production in the New Inflationary Cosmology*, *Phys. Lett.* **117B** (1982) 29.
- [38] J. H. Traschen and R. H. Brandenberger, *Particle Production During Out-of-equilibrium Phase Transitions*, *Phys. Rev. D* **42** (1990) 2491–2504.

- [39] L. Kofman, A. D. Linde, and A. A. Starobinsky, *Reheating after inflation*, *Phys. Rev. Lett.* **73** (1994) 3195–3198, [[hep-th/9405187](#)].
- [40] Y. Shtanov, J. H. Traschen, and R. H. Brandenberger, *Universe reheating after inflation*, *Phys. Rev. D* **51** (1995) 5438–5455, [[hep-ph/9407247](#)].
- [41] L. Kofman, A. D. Linde, and A. A. Starobinsky, *Towards the theory of reheating after inflation*, *Phys. Rev.* **D56** (1997) 3258–3295, [[hep-ph/9704452](#)].
- [42] B. A. Bassett, S. Tsujikawa, and D. Wands, *Inflation dynamics and reheating*, *Rev. Mod. Phys.* **78** (2006) 537–589, [[astro-ph/0507632](#)].
- [43] R. Allahverdi, R. Brandenberger, F.-Y. Cyr-Racine, and A. Mazumdar, *Reheating in Inflationary Cosmology: Theory and Applications*, *Ann. Rev. Nucl. Part. Sci.* **60** (2010) 27–51, [[arXiv:1001.2600](#)].
- [44] J. Martin and C. Ringeval, *First CMB Constraints on the Inflationary Reheating Temperature*, *Phys. Rev.* **D82** (2010) 023511, [[arXiv:1004.5525](#)].
- [45] J. Mielczarek, *Reheating temperature from the CMB*, *Phys. Rev. D* **83** (2011) 023502, [[arXiv:1009.2359](#)].
- [46] M. A. Amin, M. P. Hertzberg, D. I. Kaiser, and J. Karouby, *Nonperturbative Dynamics Of Reheating After Inflation: A Review*, *Int. J. Mod. Phys.* **D24** (2014) 1530003, [[arXiv:1410.3808](#)].
- [47] L. Dai, M. Kamionkowski, and J. Wang, *Reheating constraints to inflationary models*, *Phys. Rev. Lett.* **113** (2014) 041302, [[arXiv:1404.6704](#)].
- [48] J. Martin, C. Ringeval, and V. Vennin, *Observing Inflationary Reheating*, *Phys. Rev. Lett.* **114** (2015), no. 8 081303, [[arXiv:1410.7958](#)].
- [49] V. Domcke and J. Heisig, *Constraints on the reheating temperature from sizable tensor modes*, *Phys. Rev. D* **92** (2015), no. 10 103515, [[arXiv:1504.0034](#)].
- [50] J. L. Cook, E. Dimastrogiovanni, D. A. Easson, and L. M. Krauss, *Reheating predictions in single field inflation*, *JCAP* **1504** (2015) 047, [[arXiv:1502.0467](#)].
- [51] D. Maity and P. Saha, *Minimal inflationary cosmologies and constraints on reheating*, [arXiv:1610.0017](#).
- [52] K. D. Lozanov and M. A. Amin, *Equation of State and Duration to Radiation Domination after Inflation*, *Phys. Rev. Lett.* **119** (2017), no. 6 061301, [[arXiv:1608.0121](#)].
- [53] R. Kabir, A. Mukherjee, and D. Lohiya, *Reheating constraints on Kähler moduli inflation*, *Mod. Phys. Lett. A* **34** (2019), no. 15 1950114, [[arXiv:1609.0924](#)].
- [54] D. Maity and P. Saha, *(P)reheating after minimal Plateau Inflation and constraints from CMB*, [arXiv:1811.1117](#).
- [55] D. Maity and P. Saha, *Minimal plateau inflationary cosmologies and constraints from reheating*, *Class. Quant. Grav.* **36** (2019) 045010, [[arXiv:1902.0189](#)].
- [56] K. El Bourakadi, *Preheating and Reheating after Standard Inflation*, [arXiv:2104.1055](#).
- [57] S. D. Odintsov and T. Paul, *From inflation to reheating and their dynamical stability analysis in Gauss–Bonnet gravity*, *Phys. Dark Univ.* **42** (2023) 101263, [[arXiv:2305.1911](#)].
- [58] G. German, J. C. Hidalgo, and L. E. Padilla, *Inflationary models constrained by reheating*, *Eur. Phys. J. Plus* **139** (2024), no. 3 302, [[arXiv:2310.0522](#)].
- [59] J. B. Munoz and M. Kamionkowski, *Equation-of-State Parameter for Reheating*, *Phys. Rev. D* **91** (2015), no. 4 043521, [[arXiv:1412.0656](#)].
- [60] J. Martin and C. Ringeval, *Inflation after WMAP3: Confronting the Slow-Roll and Exact Power Spectra to CMB Data*, *JCAP* **0608** (2006) 009, [[astro-ph/0605367](#)].

- [61] P. Adshead, R. Easther, J. Pritchard, and A. Loeb, *Inflation and the Scale Dependent Spectral Index: Prospects and Strategies*, *JCAP* **02** (2011) 021, [[arXiv:1007.3748](#)].
- [62] D. Nandi and P. Saha, *Einstein or Jordan: seeking answers from the reheating constraints*, [arXiv:1907.1029](#).
- [63] A. R. Liddle and S. M. Leach, *How long before the end of inflation were observable perturbations produced?*, *Phys. Rev.* **D68** (2003) 103503, [[astro-ph/0305263](#)].
- [64] **PRISM** Collaboration, P. Andre *et. al.*, *PRISM (Polarized Radiation Imaging and Spectroscopy Mission): A White Paper on the Ultimate Polarimetric Spectro-Imaging of the Microwave and Far-Infrared Sky*, [arXiv:1306.2259](#).
- [65] **Euclid Theory Working Group** Collaboration, L. Amendola *et. al.*, *Cosmology and fundamental physics with the Euclid satellite*, *Living Rev. Rel.* **16** (2013) 6, [[arXiv:1206.1225](#)].
- [66] Y. Mao, M. Tegmark, M. McQuinn, M. Zaldarriaga, and O. Zahn, *How accurately can 21 cm tomography constrain cosmology?*, *Phys. Rev.* **D78** (2008) 023529, [[arXiv:0802.1710](#)].
- [67] **CORE** Collaboration, F. Finelli *et. al.*, *Exploring cosmic origins with CORE: Inflation*, *JCAP* **1804** (2018) 016, [[arXiv:1612.0827](#)].
- [68] J. Martin, C. Ringeval, and R. Trotta, *Hunting Down the Best Model of Inflation with Bayesian Evidence*, *Phys. Rev.* **D83** (2011) 063524, [[arXiv:1009.4157](#)].
- [69] J. Martin, C. Ringeval, R. Trotta, and V. Vennin, *The Best Inflationary Models After Planck*, *JCAP* **1403** (2014) 039, [[arXiv:1312.3529](#)].
- [70] J. Martin, C. Ringeval, and V. Vennin, *How Well Can Future CMB Missions Constrain Cosmic Inflation?*, *JCAP* **1410** (2014), no. 10 038, [[arXiv:1407.4034](#)].
- [71] M. Kaur, D. Nandi, and S. R. B, *Unifying inflationary and reheating solution*, *JCAP* **05** (2024) 045, [[arXiv:2309.1057](#)].
- [72] P. Auclair, B. Blachier, and C. Ringeval, *Clocking the End of Cosmic Inflation*, [arXiv:2406.1415](#).
- [73] Q.-G. Huang, *Slow-roll reconstruction for running spectral index*, *Phys. Rev. D* **76** (2007) 043505, [[astro-ph/0610924](#)].
- [74] C. Caprini, S. H. Hansen, and M. Kunz, *Observational constraint on the fourth derivative of the inflaton potential*, *Mon. Not. Roy. Astron. Soc.* **339** (2003) 212–214, [[hep-ph/0210095](#)].
- [75] J. M. Cline and L. Hoi, *Inflationary potential reconstruction for a wmap running power spectrum*, *JCAP* **06** (2006) 007, [[astro-ph/0603403](#)].
- [76] Q.-G. Huang and M. Li, *Running spectral index in noncommutative inflation and wmap three year results*, *Nucl. Phys. B* **755** (2006) 286–294, [[astro-ph/0603782](#)].
- [77] Q.-G. Huang, *Running of Running of the Spectral Index and WMAP Three-year data*, *JCAP* **11** (2006) 004, [[astro-ph/0610389](#)].
- [78] H. Peiris and R. Easther, *Recovering the Inflationary Potential and Primordial Power Spectrum With a Slow Roll Prior: Methodology and Application to WMAP 3 Year Data*, *JCAP* **07** (2006) 002, [[astro-ph/0603587](#)].
- [79] R. Easther and H. Peiris, *Implications of a Running Spectral Index for Slow Roll Inflation*, *JCAP* **09** (2006) 010, [[astro-ph/0604214](#)].
- [80] H. Peiris and R. Easther, *Slow Roll Reconstruction: Constraints on Inflation from the 3 Year WMAP Dataset*, *JCAP* **10** (2006) 017, [[astro-ph/0609003](#)].
- [81] K. I. Izawa, *Supergravity minimal inflation and its spectral index revisited*, *Phys. Lett. B* **576** (2003) 1–4, [[hep-ph/0305286](#)].

- [82] A. Ashoorioon, J. L. Hovdebo, and R. B. Mann, *Running of the spectral index and violation of the consistency relation between tensor and scalar spectra from trans-Planckian physics*, *Nucl. Phys. B* **727** (2005) 63–76, [[gr-qc/0504135](#)].
- [83] G. Ballesteros, J. A. Casas, and J. R. Espinosa, *Running spectral index as a probe of physics at high scales*, *JCAP* **03** (2006) 001, [[hep-ph/0601134](#)].
- [84] M. Li, *Nonminimal Inflation and the Running Spectral Index*, *JCAP* **10** (2006) 003, [[astro-ph/0607525](#)].
- [85] B. Chen, M. Li, T. Wang, and Y. Wang, *Inflation with High Derivative Couplings*, *Mod. Phys. Lett. A* **22** (2007) 1987–1994, [[astro-ph/0610514](#)].
- [86] V. Vennin, K. Koyama, and D. Wands, *Encyclopædia curvatonis*, *JCAP* **11** (2015) 008, [[arXiv:1507.0757](#)].
- [87] A. Karam, T. Pappas, and K. Tamvakis, *Frame-dependence of higher-order inflationary observables in scalar-tensor theories*, *Phys. Rev. D* **96** (2017), no. 6 064036, [[arXiv:1707.0098](#)].
- [88] A. A. Starobinsky, *The Perturbation Spectrum Evolving from a Nonsingular Initially De-Sitter Cosmology and the Microwave Background Anisotropy*, *Sov. Astron. Lett.* **9** (1983) 302.
- [89] A. A. Starobinsky and H. J. Schmidt, *On a general vacuum solution of fourth-order gravity*, *Class. Quant. Grav.* **4** (1987) 695–702.
- [90] S. Koh, B.-H. Lee, and G. Tumurtushaa, *Constraints on the reheating parameters after Gauss-Bonnet inflation from primordial gravitational waves*, *Phys. Rev.* **D98** (2018), no. 10 103511, [[arXiv:1807.0442](#)].
- [91] J. de Haro, *Reheating constraints in instant preheating*, *Phys. Rev. D* **107** (2023), no. 12 123511, [[arXiv:2304.0590](#)].
- [92] G. N. Felder, L. Kofman, and A. D. Linde, *Instant preheating*, *Phys. Rev. D* **59** (1999) 123523, [[hep-ph/9812289](#)].
- [93] **PRISM** Collaboration, P. Andre *et. al.*, *PRISM (Polarized Radiation Imaging and Spectroscopy Mission): A White Paper on the Ultimate Polarimetric Spectro-Imaging of the Microwave and Far-Infrared Sky*, [arXiv:1306.2259](#).
- [94] **Euclid Theory Working Group** Collaboration, L. Amendola *et. al.*, *Cosmology and fundamental physics with the Euclid satellite*, *Living Rev. Rel.* **16** (2013) 6, [[arXiv:1206.1225](#)].
- [95] J. M. Maldacena, *Non-Gaussian features of primordial fluctuations in single field inflationary models*, *JHEP* **0305** (2003) 013, [[astro-ph/0210603](#)].
- [96] D. Nandi and S. Shankaranarayanan, *Complete Hamiltonian analysis of cosmological perturbations at all orders*, *JCAP* **06** (2016) 038, [[arXiv:1512.0253](#)].
- [97] D. Nandi and S. Shankaranarayanan, *Complete Hamiltonian analysis of cosmological perturbations at all orders II: Non-canonical scalar field*, *JCAP* **10** (2016) 008, [[arXiv:1606.0574](#)].
- [98] D. Nandi, *Hamiltonian formalism of cosmological perturbations and higher derivative theories*, [arXiv:1707.0297](#).
- [99] D. Nandi and L. Sriramkumar, *Can a nonminimal coupling restore the consistency condition in bouncing universes?*, *Phys. Rev. D* **101** (2020), no. 4 043506, [[arXiv:1904.1325](#)].
- [100] D. Nandi, *Note on stability in conformally connected frames*, *Phys. Rev. D* **99** (2019), no. 10 103532, [[arXiv:1904.0015](#)].
- [101] D. Nandi, *Stable contraction in Brans-Dicke cosmology*, *JCAP* **05** (2019) 040, [[arXiv:1811.0962](#)].

- [102] R. Kothari and D. Nandi, *B-Mode auto-bispectrum due to matter bounce*, *JCAP* **10** (2019) 026, [[arXiv:1901.0653](#)].
- [103] D. Nandi, *Bounce from Inflation*, *Phys. Lett. B* **809** (2020) 135695, [[arXiv:2003.0206](#)].
- [104] D. Nandi, *Stability of a viable non-minimal bounce*, *Universe* **7** (2021), no. 3 62, [[arXiv:2009.0313](#)].
- [105] D. Nandi and M. Kaur, *Viable bounce from non-minimal inflation*, [arXiv:2206.0833](#).
- [106] D. Nandi and M. Kaur, *Inflation vs. Ekpyrosis — Comparing stability in general non-minimal theory*, *Phys. Dark Univ.* **44** (2024) 101430, [[arXiv:2302.0341](#)].
- [107] M. Kaur, D. Nandi, D. Choudhury, and T. R. Seshadri, *Universe bouncing its way to inflation*, *Int. J. Mod. Phys. D* **33** (2024), no. 02 2450006, [[arXiv:2302.1369](#)].